

1 Article

2 ***Cucurbita argyrosperma* seed extracts attenuate**
3 **angiogenesis in a corneal chemical burn model**4 **María Fernanda Estrella-Mendoza¹, Francisco Jiménez-Gómez², Adolfo López-Ornelas², Rosa**
5 **Martha Pérez-Gutiérrez¹, and Javier Flores-Estrada^{2,*}**6 ¹ Laboratorio de Investigación de productos naturales, Escuela de Ingeniería Química e Industrias
7 Extractivas, Instituto Politécnico Nacional. Unidad Profesional Adolfo López Mateos, Av. Instituto
8 Politécnico Nacional S/N, 07708 Ciudad de México, México; fernandaestrella29@hotmail.com;
9 rmpg@prodigy.net.mx10 ² División de Investigación, Hospital Juárez de México. Av. Instituto Politécnico Nacional 5160, Magdalena
11 de las Salinas, Gustavo A. Madero, 07760, Ciudad de México, México; jose.florese@salud.gob.mx

12 * Correspondence: jose.florese@salud.gob.mx; Tel.: +52-55-5747-7560 (ext.7476)

13 Received: date; Accepted: date; Published: date

14 **Abstract:** Cornea severe inflammation produces opacity or even perforation, scarring, and
15 angiogenesis, resulting in blindness. The cornea can be used to study the effect of new anti-
16 angiogenic chemopreventive agents. We researched the anti-angiogenic effect of two extracts,
17 Methanol (Met) and Hexane (Hex), from the seed of *Cucurbita argyrosperma*, in the inflamed corneas.
18 The corneas of Wistar rats were alkali-injured and treated intragastrically for seven successive days.
19 Clinical manifestation as opacity score, corneal neovascularization (CNV) area, re-epithelialization
20 percentage, and histological evaluation were performed. Inflammatory (COX-2, NF- κ B, and IL-1 β),
21 and angiogenic (VEGF-A, VEGFR1, VEGFR2) markers were assessed by immunohistochemistry.
22 Cox-2, Il-1 β , and Vegf-a mRNA levels were also determined. After treatments, we observed slim
23 corneal thickness with lower opacity scores and low cell infiltration compared to untreated rats.
24 Treatment also accelerated wound healing and decreased CNV area. The staining of inflammatory
25 and angiogenic factors was significantly decreased. These effects are related to a down-expression
26 of Cox-2, Il-1 β , and Vegf. These results suggest that intake of *C. argyrosperma* seed can be used to
27 attenuate the angiogenesis secondary to inflammation in corneal chemical damage.28 **Keywords:** *C. argyrosperma*; corneal chemical burn; angiogenesis; corneal neovascularization (CNV);
29 Vascular Endothelial Growth Factor (VEGF); Interleukin-1 β (IL-1 β); Cyclooxygenase-2 (COX-2);
30 Nuclear Factor-kappaB (NF- κ B).32 **1. Introduction**33 Angiogenesis, the formation of new blood vessels from the pre-existing ones, inflammation, and
34 oxidative stress are important factors that predispose and promote the progression of degenerative
35 diseases such as tumors and diabetes, and corneal diseases are not an exception. Corneal
36 neovascularization (CNV), caused by viral infections, autoimmune diseases, and chemical burns
37 could progress into defective healing with persistent perforation and ulceration, resulting in
38 blindness or failure in the penetrating keratoplasty when not treated in a timely manner [1]. Under
39 this condition, NF- κ B signaling pathway in inflammatory, epithelial, and endothelial cells, is a key
40 step for the transcriptional overexpression of pro-inflammatory and proangiogenic factors, including
41 interleukin-1 β (IL-1 β), cyclooxygenase 2 (COX-2), and vascular endothelial growth factor A (VEGF-
42 A). COX-2 enzyme increases the synthesis of prostaglandins to modulate cell proliferation, cell death,
43 and tumor invasion in many types of cancer. IL-1 β , IL-6 or TNF- α , regulate COX-2, therefore, they
44 are overexpressed during inflammation [2-4].

45

46 In the alkali-burn corneal injury, VEGF-A is an important factor of angiogenesis when is
47 expressed in macrophages and epithelial cells. VEGF-A binds to two main tyrosine kinase receptors,
48 VEGFR1 and VEGFR2, on the vascular endothelial cell to promote migration, proliferation, and
49 formation of capillaries, along with monocyte/macrophage migration in the microenvironment
50 injured [1,5,6]. Several therapeutic strategies to reduce CNV are studied based on these observations,
51 topical or subconjunctival treatments, mainly corticosteroids and non-steroidal anti-inflammatory
52 agents [7], have limited use and potential side effects as an impediment of wound healing [8,9]. Anti-
53 VEGF therapy in chemically burned ocular tissues results in a substantial reduction of angiogenesis
54 both animal studies and clinical trials [10,11]. However, to establish its safety and efficacy, controlled
55 and randomized trials to justify their continued use are required. Besides, systemic drug treatment is
56 not recommended because of adverse effects. Thus, it is important the search for new drugs for the
57 systemic treatment of these disorders.
58

59 Current data in CNV models shown that natural extracts from plants or the bioactive
60 compounds in its extracts have angiogenic suppressing activity [12-14]. The genus *Cucurbita*
61 (pumpkin) belongs to one of the 300 genera of the Cucurbitaceae family and it is one of the most
62 popular vegetables eaten in the world. Recently, pumpkin was recognized as a functional food and
63 *Cucurbita pepo*, *C. maxima*, *C. moschata*, *C. andreana*, and *C. ficifolia* are the most cultivated species [15].
64 Nutritionally, pumpkin seed contains a high amount of polyunsaturated fatty acids as well as
65 proteins, vitamins, several minerals, and other phytochemicals. The anti-diabetic, antioxidant, anti-
66 carcinogenic, anti-inflammatory properties of this seed are studied due to its high content natural
67 bioactive compounds, such as carotenoids, tocopherols, and sterols [16-19].
68

69 *Cucurbita argyrosperma* is an economically important species cultivated in Mesoamerica.
70 Isozyme, morphological, and ecological analysis suggest that it was probably domesticated from the
71 Mexican wild squash *C. sororia* [20]. Seed is usually consumed as a snack or as an ingredient in
72 traditional stews, although the scientific findings of its beneficial effects on human health have not
73 been sufficiently proven and the anti-neovascular effects of the secondary metabolites remain
74 unknown. However, conceivably its phytochemical composition could be like the related species,
75 showing anti-inflammatory effects as suggested. Besides, proangiogenic factors such as COX-2, IL-
76 1 β , and, VEGF, including to VEGFR1 and -R2, induced by the inflammatory agents has not studied
77 these plants.
78

79 The aim of this study was to contribute with new evidence of the effect of seed extracts from *C.*
80 *argyrosperma* in the inflammatory and angiogenic process attenuation. Here show that hexanic and
81 methanolic extracts from *C. argyrosperma* seed significantly attenuates the expression of
82 proangiogenic factors during the inflammation using CNV model. Also, we observed by clinical
83 manifestation that both extracts significantly diminish corneal neovascularization area. Remarkably,
84 corneal re-epithelialization was higher in the hexane extract treatment than methanol extract.
85

86 2. Materials and Methods

87 2.1 Extract Preparation

88 The pumpkins of *C. argyrosperma* were harvested in an agricultural field of the Michoacán
89 Province, México and identified by a botanist in the herbarium of The National Polytechnic Institute
90 (IPN). Voucher specimen number 4532 was deposited in the herbarium of the National School of
91 Biological Sciences of IPN. One kilogram of seed was extracted with 3L of hexane (50% v/v) and left
92 to macerate for 8 days at room temperature. Crude extract was filtered for one hour in 8 μ M-medium
93 flow filter paper (Whatman®), concentrated using a rotary vacuum evaporator and taken to dryness
94 at 60°C in a vacuum rotator until the complete removal of the solvent, obtaining a viscous residue
95

96 (8.38 g/L). The same procedure was applied to the residue, using methanol for a sequential separation
97 of the seed components. Each extract was stored in the dark at 4°C until use.
98

99 2.2 Animal model

100 Twenty-eight male Wistar rats weighing 200-250 g were used. Water and standard food were
101 available *ad libitum*. The care and management of experimental animals were performed according
102 to the guidelines of the National Institutes of Health Guide for the Care and Use of Laboratory
103 Animals, the standards described by ARVO (Association for Research in Vision and Ophthalmology),
104 and Official Mexican Standard NOM-062-ZOO-1999.
105

106 2.3 Experimental design

107 Each extract was dissolved in 0.5 ml (water) and Tween-80 (20%), which was also used as the
108 vehicle (Veh). Rats were randomly divided into four groups (n=7 each): Non-chemically burned
109 healthy corneas (Non-CB) treated only with the vehicle; chemically burned (CB) corneas treated with
110 the vehicle (CB-Veh); hexanic extract treatment (CB-Hex); and methanolic extract treatment (CB-
111 Met). Groups were intragastrically injected with 400 mg/kg of Hex/Met extracts or 0.5 ml of the
112 vehicle in a single dose, at the same time daily (10:00 am). 48h later, animals were intraperitoneally
113 anesthetized with pentobarbital sodium (0.5 mg/kg), inhaled sevoflurane, and one drop of
114 ophthalmic tetracaine, to perform the chemical cauterization of the cornea. Central corneas from the
115 right eyes were burned by applying a 3-mm-diameter filter paper saturated with 1M NaOH solution
116 for 30 seconds and immediately washing with 10 ml of saline solution. To avoid infection, a drop of
117 ophthalmic ciprofloxacin was applied every 24 hours until the end of the study. Animals were
118 euthanized with an overdose of pentobarbital.
119

120 2.4 Clinical manifestation

121 Corneal opacity, epithelial defects, and the CNV area were clinically evaluated eight days after
122 CB. Corneal opacity was scored using a scaling system from 0 to 4: 0=no opacity, completely clear
123 cornea; 1=slightly hazy, iris and lens visible; 2=moderately opaque, iris and lens still detectable;
124 3=severely opaque, iris and lens hardly visible; and 4=completely opaque, with no visibility of the iris
125 and lens [21].
126

127 The measurement of the CNV area (mm²) was performed *in vivo* using a ruler under a
128 microscope and photographed. The software program Image-Pro Plus version 6.0 software (by Media
129 Cybernetics, Inc., Rockville, MD, USA) was used. Inferonasal quadrant was selected to calculate the
130 neovascularized area, according to previous reports [22].
131

132 To evaluate corneal wound re-epithelialization, we used corneal fluorescein staining. Briefly, the
133 lateral conjunctival sac was stained using fluorescein sodium ophthalmic strips. Corneas were
134 examined using a slit lamp biomicroscope with cobalt blue light. Injured epithelial tissues retain the
135 fluorescein staining, meanwhile, the lack of stain indicates a re-epithelialization. The re-
136 epithelialization percentage was evaluated from corneal central burning, considering that a total area
137 of approx. 7 mm² is 100 percent (3 mm disc 1M NaOH-embedded).
138

139 2.5 Histological evaluation

140 Enucleated eyes (n=4 by group) were immediately fixed in neutral formalin. Cut tissue slides (3-
141 5 mm) were made, anteroposterior, and included the optic nerve. Slides were dehydrated in graded
142 alcohols and embedded in paraffin. Histological sections of 2 μ m were processed and stained with
143 hematoxylin-eosin (H&E). We measured the corneal thickness and cell infiltration in the peripheral
144 region (500 μ m beyond the limbus area) using light microscopy (axioscope 2 plus, Carl Zeiss). The
145 percentage of the infiltration was calculated in a masked fashion based on the density in the corneal
146 stroma of CB-Veh group.
147

148 Other 2 μ m-sections were dewaxed and rehydrated up to antigen recovery solution
149 (ImmunoDNA Retriever 20X with Citrate; BioSB). Slides were then loaded into a Shandon Sequenza
150 chamber (Thermo Fisher Scientific, Inc). We used the procedure described for the polymer-based
151 immunodetection system (PolyVue® mouse/rabbit DAB detection system, Diagnostic BioSystems,
152 Pleasanton, CA, USA). We applied 100 μ l of IL-1 β (Cat. No. sc-7884), NF- κ B p65 (sc-8008), COX-2 (sc-
153 1746), VEGF-A (sc-7269), VEGFR1 (sc-31173). All antibodies were purchased from Santa Cruz
154 Biotechnology, Inc. (Santa Cruz, CA, USA). VEGFR2 antibody (MAB3571) was purchased from R&D
155 systems. All dilutions were at 1:200 and incubated overnight at 4°C. Later, the enhancers Polyvue
156 Plus and HRP were added and incubated with DAB plus/chromogen substrate and counterstained
157 hematoxylin. An Axio Imager.A2 microscope with an integrated camera (axiocam ICc5; Carl Zeiss
158 Microscopy GmbH, Germany) was used for histological observation and image capture. Micrographs
159 of the peripheral region of the cornea (3 fields per side and 500 mm above the limb, at 200X of
160 magnitude) were taken to measure the mean staining intensity of these markers. Images were
161 analyzed with the Image-Pro Plus software version 6.0.
162

163 2.6 Quantitative-reverse-transcription polymerase chain reaction (qRT-PCR)

164 Total RNA was isolated from corneal tissue using TRIzol™ Reagent (Invitrogen, Boston, MA,
165 USA) (n=3 by group). One microgram of DNase I-treated RNA (Roche Applied Science, Germany)
166 was reverse transcribed with SuperScript® II Reverse Transcriptase system. Quantification of mRNA
167 was carried out using qPCR with SYBR green and the following primers: Cox-2 (5'-
168 CTGAGGGGTTACCACTTCCA-3'; and 5'-CTTGAACACGGACTTGCTCA-3'); Il-1 β (5'-
169 AGGCTTCCTTGTGCAAGTGT-3' and 5'-TGAGTGACACTGCCTCCTG-3'); Vegf-a (5'-
170 GCCCATGAAGTGGTGAAGTT-3' and 5'-ACTCCAGGGCTTCATCATTG-3'); and Gapdh (5'-
171 CTCATGACCACAGTCCATGC-3' and 5'-TTCAGCTCTGGATGACCTT-3'). The cycling protocol was
172 as follows: denaturation (95°C for 10 min), 45 cycles of amplification (95°C for 15 s, 59°C for 15 s, and
173 72 °C for 20 s), and a final extension at 72°C. A melting curve analysis was also performed to ascertain
174 the specificity of the amplified product. The expression for each gene was normalized to Gapdh.
175 Expression was quantified as fold-change using the $\Delta\Delta Ct$ method.
176

177 2.7 Statistical analysis

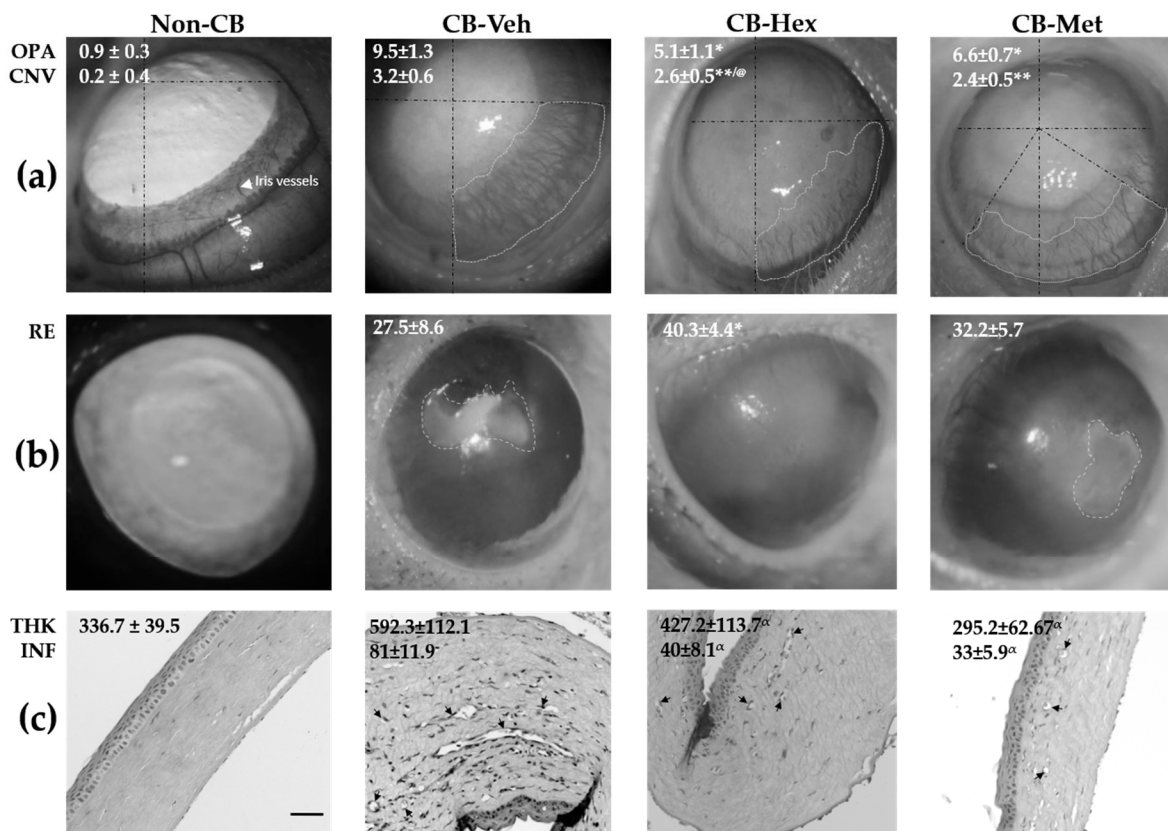
178 We used GraphPad Prism software (La Jolla, CA, USA) (version 5.0). Values are mean with
179 standard deviation (mean \pm SD). In all cases, we used unifactorial analysis of variance followed by
180 Tukey's *post hoc* analysis.
181

182 3. Results

183 3.1 Amelioration of corneal wound repair

184 We evaluated corneal wound healing mediated by the extracts in the alkali-burn corneal model.
185 Figure 1a shows that treated groups had a significant reduction in corneal opacity score and CNV
186 area compared to CB-Veh ($p<0.05$ and $p<0.001$, respectively). However, CNV in CB-Met was lower
187 than CB-Hex treatment ($p<0.05$). Furthermore, CB-Met does not show significant differences in the
188 percentage of re-epithelialization compared to CB-Veh, inverse to CB-Hex treatment (Figure 1b).

189 H&E stained slides (Figure 1c), non-CB group had an average corneal thickness, 336.7 \pm 39.5 μ m,
190 with integral epithelial layers and a dense stroma, consisting of keratocytes. There are neither
191 inflammatory cells nor blood vessels. Conversely, corneal integrity in CB-Veh group was severely
192 impaired, with the loss of the epithelial cell layers, an extreme denaturation of stromal collagen fibers,
193 and an average cell infiltration of 81 \pm 11.9%. Corneal thickness was 592.3 \pm 112.1 μ m. Whereas, CB-Hex
194 tissues display a 40 \pm 8.1% infiltration, with a corneal thickness of 427.2 \pm 113.7 μ m ($p<0.001$ compared
195 to CB-Veh). In CB-Met group, there is a significant decrease in cell infiltration (33.2 \pm 5.9%) and
196 thickness of 295.2 \pm 62.67 μ m ($p<0.001$ compared to CB-Veh), but corneal thickness in CB-Met no shown
197 difference with Non-CB.

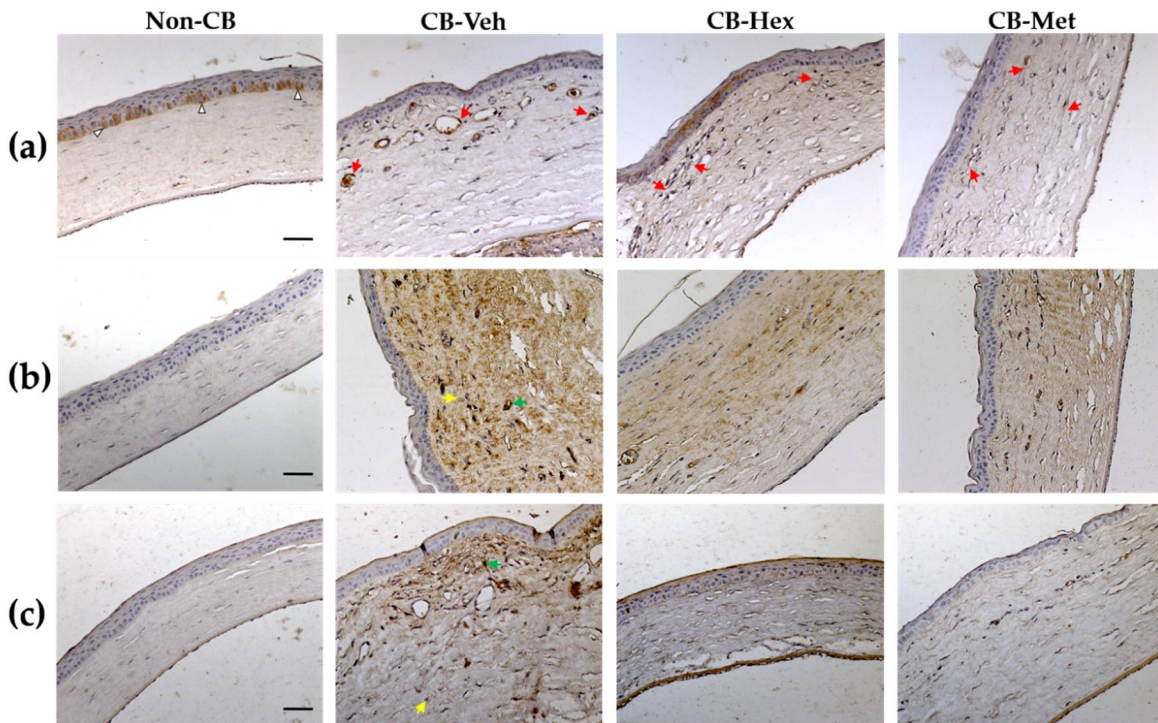
198
199

200 **Figure 1.** Methanol (Met) and hexane (Hex) extracts of *C. argyrosperma* seed in alkali-injured corneas
 201 (CB) compared to the untreated group (CB-Veh). **(a)** average of opacity score (Opa) and corneal
 202 neovascularization area (CNV) in mm². **(b)** re-epithelialization percentage (RE) and **(c)** corneal
 203 thickness in microns (THK) and infiltration cell percentage (INF). Average value ± SD; *p < 0.05;
 204 **p < 0.01, and ^αp < 0.001 compared to CB-Veh. [◎]p < 0.05 compared to CB-Met. Gray dotted lines show studied
 205 area and black lines are geometrical axis. Arrows indicate the lumen of stromal blood vessels. (Scale
 206 bar = 100 μ m).

207 **2 Anti-inflammatory effect**

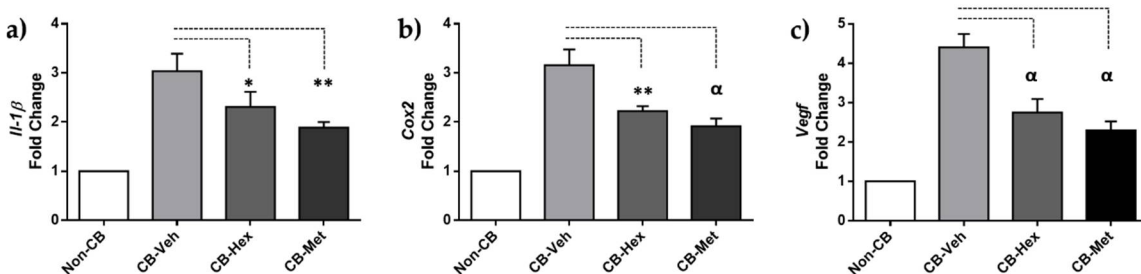
208 Several inflammatory cytokines implicated in alkali-induced corneal injury are regulated by the
 209 nuclear internalization of active NF- κ B. Hence, we glance for the staining location of NF- κ B in the
 210 corneal lesions. In Non-CB, NF- κ B was restricted in the cytoplasm of epithelial cells in the basal layer
 211 (Figure 2a). In CB-Veh and both extracts-treated groups, NF- κ B was distributed in the nuclear
 212 compartment of endothelial and inflammatory cells. However, staining density decreased in CB-Hex
 213 (41.13 ± 9.6) and CB-Met (32.73 ± 8.1) compared to CB-Veh (73.31 ± 10.4; p < 0.0001 both). Additionally, we
 214 performed measurements of the staining intensity for IL-1 β (Figure 2b) and COX-2 (Figure 2c). In
 215 Non-CB there was a low staining intensity for IL-1 β (9.28 ± 2.6) compared to CB-Veh (75.95 ± 12.16;
 216 p < 0.0001), showing a distribution along the corneal stroma, as well as endothelial cells. Meanwhile,
 217 the intensities in CB-Hex (42.16 ± 9.14) and CB-Met (38.21 ± 7.9) were lower than CB-Veh group
 218 (p < 0.0001). Staining intensity for IL-1 β between CB-Met and CB-Hex have no differences (p > 0.5).
 219 Likewise, the intensity for COX-2 was significantly different when comparing CB-Veh (102.6 ± 13.08)
 220 to CB-Hex (68.79 ± 10.73) and CB-Met (37.15 ± 7.18) (p < 0.0001). Non-CB has a detectable expression of
 221 7.49 ± 3.48. Staining intensity for IL-1 β and COX-2 in the cornea was also confirmed at the level of
 222 mRNA (Figure 3). *Il-1 β* expression for CB-Met (2.31 ± 0.30) and CB-Hex (1.89 ± 0.11) was decreased
 223 compared to CB-Veh (3.03 ± 0.35; p < 0.05 and p < 0.01, respectively) (Figure 3a). *Cox-2* in CB-Hex
 224 (2.22 ± 0.10) and CB-Met (1.91 ± 0.15) was also diminished compared to Veh (3.15 ± 0.31; p < 0.01) (Figure

225 3b). The *Il-1 β* expression had not differences between CB-Met and CB-Hex ($p>0.5$), on the other hand,
226 there was for *Cox-2* ($p<0.05$).



227

228 **Figure 2.** Micrograph of Met and Hex extracts of *C. argyrosperma* seed in CB compared to non-CB-
229 Veh. (a) Nuclei stained with anti-NF- κ B p65 (red arrows). (b) Staining intensity for IL-1 β along the
230 corneal thickness. (c) COX-2 staining in studied groups. Arrowheads indicate the cytoplasmic
231 distribution of NF- κ B p65. Yellow and green arrows represent the minimum and maximum,
232 respectively, staining intensity considered for software analysis. (Scale bar = 100 μ m).



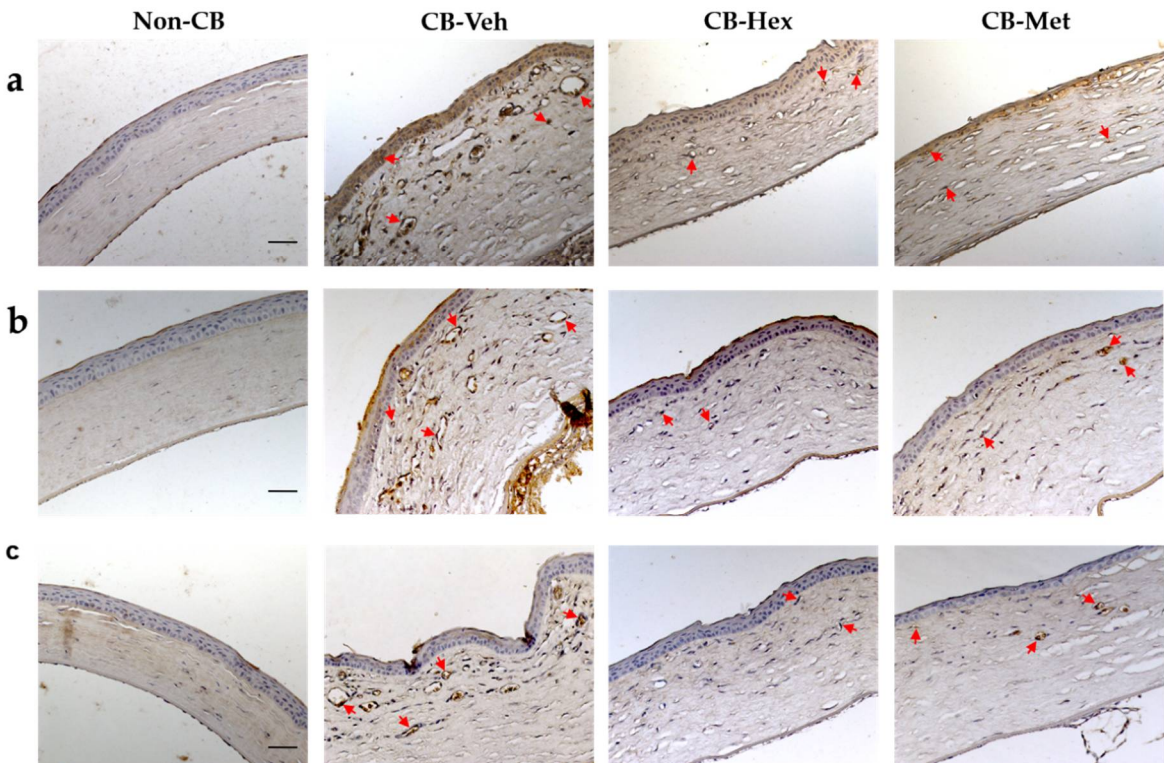
233

234 **Figure 3.** qRT-PCR for *Il-1 β* (a), *Cox-2* (b), and *Vegf-a* (c). Bars are the expression levels in each group.
235 * $p\leq 0.05$, ** $p\leq 0.01$, and $\alpha p\leq 0.001$ compared to CB-Veh.

236 3.3 Anti-angiogenic effect

237 Due to the anti-inflammatory effect in CB-Hex and CB-Met, we assessed whether it was related
238 to an attenuation of CNV, by determining the staining intensity of VEGF-A and its receptors (Figure
239 4). In CB-Veh, VEGF-A was in the cytoplasm and nucleus of the epithelial, endothelial and other
240 infiltrated cells with an intensity of 102.02 ± 14.04 . Decreased on VEGF-A intensities were observed for
241 CB-Hex (71 ± 9.11) and CB-Met (61.3 ± 9.59) ($p<0.001$). Besides, staining intensity between VEGF-A in
242 CB-Met and CB-Hex show differences ($p<0.05$) and in Non-CB, this was about 16.25 ± 5.25 (Figure 4a).
243 *Vegf-a* expression was also confirmed (Figure 3c). *Vegf-a* for CB-Hex (2.74 ± 0.34) and CB-Met
244 (2.29 ± 0.23) was decreased compared to CB-Veh (4.40 ± 0.34 ; $p<0.05$ and $p<0.01$, respectively).

245 Relevantly, staining for VEGFR1 was distributed in endothelial and inflammatory cells of CB-
 246 Veh corneas (54.4 ± 6.8) and was higher as compared to CB-Hex (33.13 ± 5.8 ; $p < 0.0001$) and to CB-Met
 247 (25.47 ± 3.7 ; $p < 0.0001$) (Figure 4b). VEGFR2 immunostaining was localized in the membrane region in
 248 endothelial cells and in CB-Veh (23.06 ± 3.5) was higher compared to CB-Hex (15.67 ± 2.6 ; $p < 0.0001$) and
 249 CB-Met (10.95 ± 2.1 ; $p < 0.0001$) (Figure 4c).



250

251 **Figure 4.** Immunolocalization of VEGF-A and its receptors, VEGFR and VEGFR2, in treated groups.
 252 (a) Staining intensities for VEGF-A. (b and c) Membranous staining in endothelial cells for VEGFR1
 253 and VEGFR2, respectively (red arrows). Red arrows represent staining intensity considered for
 254 software analysis. (Scale bar = 100 μ m).

255

256 4. Discussion

257 The cornea is a transparent, avascular and immune privileged tissue. However, the inflammatory
 258 response and growth of neovessels induced by infections, autoimmunity, and chemical burn may
 259 cause vision loss and high rejection rate of corneal allografts if not treated effectively [1,23]. Currently,
 260 it has been demonstrated by histopathological and clinical findings in animal models that anti-
 261 neovascular topical treatments are successful to avoid CNV [8,24]. Nonetheless, its regulatory
 262 mechanisms are just starting to be understood. To examine this phenomenon, experimental models
 263 combined with new therapeutic strategies have been planned, primarily aimed to preserve corneal
 264 transparency through epithelial integrity by attenuating the inflammatory and neovascularization
 265 responses.

266

267 Chemically burned corneas has long been used for this purpose because is accompanied by the
 268 recruitment/migration of neutrophils and macrophages with the resultant damage to the normal
 269 tissue structure, conducted by the release of oxidative derivatives, cytokines, and chemokines, matrix
 270 metalloproteinases (MMPs), and growth factors, including to VEGF can influence corneal
 271 angiogenesis [25–27]. Topical treatments with monoclonal antibody anti-VEGF- or their receptor
 272 VEGFR2 suppress the mechanism of action of VEGF in endothelial cell. Whereas dexamethasone

273 inhibits CNV mediated by suppressing the activity of NF- κ B, decreasing the expression of IL-1 β and
274 COX-2, and VEGF [28]. In the same way, treatments with extracts of Propolis and *Diospyros kaki*; as
275 well as other purified phytochemicals (Naringenin and EGCG) shown a decrease CNV through
276 down-regulation of VEGF-A, IL-1 β , IL-6, and metalloproteases, promoting corneal wounds healing
277 [12-14].
278

279 In the present study, we aim to evidence the ability of the hexane and methanol extracts of *C.*
280 *argyrosperma* seed to reduce CNV after an inflammatory stimulus induced by chemical burn in rat
281 cornea. To this goal, we examined the nuclear localization of NF- κ B p65, an important marker for the
282 overexpression of VEGF-A, IL-1 β and COX-2 in damaged corneas. Receptor VEGFR2 in endothelial
283 cell of corneal stromal neovessels as an active marker of the angiogenesis was studied. Angiogenesis
284 initiate when VEGFR2 is activated by tyrosine phosphorylation by VEGF-A binding. Consecutively,
285 downstream pathways are activated such as p38 MAPK and ERK1/2, producing a strong mitogenic
286 and survival process [29,30]. In contrast, such a mitogenic signal is not equally induced by VEGFR1.
287 Although VEGFR1 binds to VEGF-A with higher affinity than VEGFR2, the induction of VEGFR1
288 phosphorylation is low and its downstream signaling is still poorly explored [31]. VEGFR1 possesses
289 anti-angiogenic activity by avoiding the union between VEGF-A and VEGFR2. Corneal studies show
290 that the proteolytic enzyme, MMP14, can shave the extracellular domain of VEGFR1, converting it
291 into the receptor soluble (VEGFRs) that acts as a decoy for VEGF-A [32]. Nevertheless, VEGFR1
292 indirectly induces angiogenesis by stimulating the migration of monocytes and macrophages
293 directed towards the damaged microenvironment. For these reasons, this study evaluates both
294 receptors because they are expressed predominantly in endothelial cells in the angiogenic
295 environment: (1) VEGFR1 as a marker in the infiltration of monocytes and neovessels and (2) VEGFR2
296 as an active marker of angiogenesis. Our results show that the staining intensity and the expression
297 of *Vegf-a* decreased along with the staining of VEGFR2 and VEGFR1 in endothelial cells of extract-
298 treated corneas. Additionally, the decrease of *Il-1 β* and *Cox-2* expressions were also observed,
299 suggesting that hexanic- and methanolic-extract components can attenuate these pro-angiogenic
300 factors, likely through a lack of nuclear activation of NF- κ B, which was also observed.
301

302 Treatment with hexanic extract of *C. argyrosperma* seed shows a repairing of the corneal
303 damage associated with a decrease in the expression of inflammatory and angiogenic factors. *C. pepo*
304 seed extracts, containing majorly linoleic (ALA), linolenic acids (LA), tocopherols, and sterols,
305 showed effective healing skin wounds with a complete re-epithelialization, organization of collagen
306 fibers, and absence of inflammatory cells [18]. Particularly, treatment with ALA, in cultures of corneal
307 epithelial cells and when is topically applied to a dry eye animal model, has an anti-inflammatory
308 activity by decreasing the release and the expression of inflammatory factors (TNF- α , IL-6, IL-1 β , and
309 IL-8) regulated by NF- κ B pathway [33,34]. In addition, LA decreased corneal fluorescein staining and
310 was associated with a significant decrease in the number of CD11b(+) cells [35].
311

312 Although we are still characterizing the bioactive compounds in the methanolic extract, we can
313 speculate that the content of phytochemicals is similar to the *C. pepo* seed [16]. Some of these
314 components include flavonoids as quercetin, luteolin, and apigenin which at low concentration
315 intake has a protective anti-inflammatory effect on human retinal pigment epithelial damage by
316 hypoxia, inhibiting VEGF and the factors related to its activation [36]. For example, quercetin inhibits
317 the production of inflammatory factors in VEGF-stimulated retinal photoreceptor cells, associated
318 with inactivation of NF- κ B as a consequence of the blockage of mitogen-activated protein kinases
319 (MAPK) and protein kinase B (Akt) phosphorylation [37]. Nonetheless, *C. argyrosperma* may differ in
320 the content and types of flavonoids from *C. pepo*. This would bring us closer to a better understanding
321 of the mechanisms of attenuated angiogenesis by the phytochemicals contained in the methanol
322 extract, which in turn could act synergistically, either directly or indirectly, in VEGF-A regulation.
323

324 Corneal inflammation eventually causes vision loss due to CNV. Corneal alkali-injury not only
325 raised to NF- κ B, IL-1 β , and COX-2 expression, but also significantly increase VEGF and their
326 receptors VEGFR1 and VEGFR2 in endothelial cells. This work demonstrates for the first time, that
327 methanolic or hexanic extracts of *C. argyrosperma* seed (400 mg/kg/7d) improves the healing of corneal
328 wound injured by a chemical agent and may contribute to the anti-inflammatory properties of the
329 phytochemicals in its composition. In addition, a significant reduction of the CNV was related to the
330 attenuation of proangiogenic factors. Significantly, our results indicate that *C. argyrosperma* Hex-
331 extract is better than Met-extract to reduce the corneal re-epithelialization time, improving the
332 healing process and thus preventing the entrance of microorganisms and inflammatory mediators
333 into the deeper layers, probably through the inhibition of the NF- κ B pathway during at least seven
334 days after corneal alkali-burn.

335

336 Consequently, ingestion of the seed can be an option to prevent the corneal angiogenesis. As
337 well, it might benefit wound healing or inhibit neovascularization in other degenerative pathologies.
338 Further pharmacological and phytochemical studies are required to identify its constituents and
339 accurately assess this activity.

340

341 **Author Contributions:** Conceptualization, R.M.P-G; Formal analysis, J.F-E; Investigation, M.F.E-M,
342 F. J-G, R.M.P-G and J.F-E; Methodology, M.F.E-M, F. J-G and R.M.P-G; Project administration, J.F-E;
343 Resources, F. J-G and R.M.P-G; Supervision, J.F-E; Visualization, A.L-O and J.F-E; Writing – original
344 draft, A.L-O and J.F-E; Writing – review & editing, A.L-O and J.F-E.

345

346 **Funding:** This research received no external funding

347 **Acknowledgments:** We thank Julia D. Toscano-Garibay for her numerous comments on the
348 manuscript. This research supported by the Juárez of México Hospital and School of Chemical
349 Engineering and Extractive Industries from the National Polytechnic Institute.

350 **Conflicts of Interest:** The authors declare no conflict of interest.

351

352

References

1. Azar, D.T. Corneal angiogenic privilege: angiogenic and antiangiogenic factors in corneal avascularity, vasculogenesis, and wound healing (an American Ophthalmological Society thesis). *Trans Am Ophthalmol Soc* **2006**, *104*, 264-302.
2. Kuwano, T.; Nakao, S.; Yamamoto, H.; Tsuneyoshi, M.; Yamamoto, T.; Kuwano, M.; Ono, M. Cyclooxygenase 2 is a key enzyme for inflammatory cytokine-induced angiogenesis. *FASEB journal : official publication of the Federation of American Societies for Experimental Biology* **2004**, *18*, 300-310, doi:10.1096/fj.03-0473com.
3. Nakao, S.; Kuwano, T.; Tsutsumi-Miyahara, C.; Ueda, S.; Kimura, Y.N.; Hamano, S.; Sonoda, K.H.; Saijo, Y.; Nukiwa, T.; Strieter, R.M., et al. Infiltration of COX-2-expressing macrophages is a prerequisite for IL-1 beta-induced neovascularization and tumor growth. *The Journal of clinical investigation* **2005**, *115*, 2979-2991, doi:10.1172/jci23298.
4. Sobolewski, C.; Cerella, C.; Dicato, M.; Ghibelli, L.; Diederich, M. The role of cyclooxygenase-2 in cell proliferation and cell death in human malignancies. *Int J Cell Biol* **2010**, *2010*, 215158, doi:10.1155/2010/215158.
5. Cursiefen, C.; Chen, L.; Borges, L.P.; Jackson, D.; Cao, J.; Radziejewski, C.; D'Amore, P.A.; Dana, M.R.; Wiegand, S.J.; Streilein, J.W. VEGF-A stimulates lymphangiogenesis and hemangiogenesis in inflammatory neovascularization via macrophage recruitment. *The Journal of clinical investigation* **2004**, *113*, 1040-1050, doi:10.1172/jci20465.
6. Sivak, J.M.; Ostriker, A.C.; Woolfenden, A.; Demirs, J.; Cepeda, R.; Long, D.; Anderson, K.; Jaffee, B. Pharmacologic uncoupling of angiogenesis and inflammation during initiation of pathological corneal neovascularization. *J Biol Chem* **2011**, *286*, 44965-44975, doi:10.1074/jbc.M111.294967.
7. Nakao, S.; Hata, Y.; Miura, M.; Noda, K.; Kimura, Y.N.; Kawahara, S.; Kita, T.; Hisatomi, T.; Nakazawa, T.; Jin, Y., et al. Dexamethasone inhibits interleukin-1beta-induced corneal neovascularization: role of nuclear factor-kappaB-activated stromal cells in inflammatory angiogenesis. *The American journal of pathology* **2007**, *171*, 1058-1065, doi:10.2353/ajpath.2007.070172.
8. Gupta, D.; Illingworth, C. Treatments for corneal neovascularization: a review. *Cornea* **2011**, *30*, 927-938, doi:10.1097/ICO.0b013e318201405a.
9. Sheppard, J.D.; Comstock, T.L.; Cavet, M.E. Impact of the Topical Ophthalmic Corticosteroid Loteprednol Etabonate on Intraocular Pressure. *Advances in therapy* **2016**, *33*, 532-552, doi:10.1007/s12325-016-0315-8.
10. Al-Debasi, T.; Al-Bekairy, A.; Al-Katheri, A.; Al Harbi, S.; Mansour, M. Topical versus subconjunctival anti-vascular endothelial growth factor therapy (Bevacizumab, Ranibizumab and Aflibercept) for treatment of corneal neovascularization. *Saudi journal of ophthalmology : official journal of the Saudi Ophthalmological Society* **2017**, *31*, 99-105, doi:10.1016/j.sjopt.2017.02.008.
11. Zhou, C.; Robert, M.C.; Kapoulea, V.; Lei, F.; Stagner, A.M.; Jakobiec, F.A.; Dohlman, C.H.; Paschalidis, E.I. Sustained Subconjunctival Delivery of Infliximab Protects the Cornea and Retina Following Alkali Burn to the Eye. *Invest Ophthalmol Vis Sci* **2017**, *58*, 96-105, doi:10.1167/iovs.16-20339.
12. Keshavarz, M.; Mostafaie, A.; Mansouri, K.; Shakiba, Y.; Motlagh, H.R. Inhibition of corneal neovascularization with propolis extract. *Archives of medical research* **2009**, *40*, 59-61, doi:10.1016/j.arcmed.2008.10.004.
13. Oguido, A.; Hohmann, M.S.N.; Pinho-Ribeiro, F.A.; Crespicio, J.; Domiciano, T.P.; Verri, W.A., Jr.; Casella, A.M.B. Naringenin Eye Drops Inhibit Corneal Neovascularization by Anti-Inflammatory and Antioxidant Mechanisms. *Invest Ophthalmol Vis Sci* **2017**, *58*, 5764-5776, doi:10.1167/iovs.16-19702.
14. Yang, S.J.; Jo, H.; Kim, K.A.; Ahn, H.R.; Kang, S.W.; Jung, S.H. Diospyros kaki Extract Inhibits Alkali Burn-Induced Corneal Neovascularization. *Journal of medicinal food* **2016**, *19*, 106-109, doi:10.1089/jmf.2014.3404.
15. Kocyan, A.; Zhang, L.B.; Schaefer, H.; Renner, S.S. A multi-locus chloroplast phylogeny for the Cucurbitaceae and its implications for character evolution and classification. *Molecular phylogenetics and evolution* **2007**, *44*, 553-577, doi:10.1016/j.ympev.2006.12.022.

404 16. Seun F. Akomolafe; Ganiyu Oboh; Sunday I. Oyeleye; Olorunfemi R. Molehin; Opeyemi B.
405 OgunsuyiPeiretti, P.G. Phenolic Composition and Inhibitory Ability of Methanolic Extract from
406 Pumpkin (*Cucurbita pepo* L) Seeds on Fe-induced Thiobarbituric acid reactive species in Albino Rat's
407 Testicular Tissue In-Vitro. *Journal of Applied Pharmaceutical Science* 2016, 6, 115-120,
408 doi:10.7324/JAPS.2016.60917

409 17. Yadav, M.; Jain, S.; Tomar, R.; Prasad, G.B.; Yadav, H. Medicinal and biological potential of
410 pumpkin: an updated review. *Nutrition research reviews* 2010, 23, 184-190,
411 doi:10.1017/s0954422410000107.

412 18. Bardaa, S.; Ben Halima, N.; Aloui, F.; Ben Mansour, R.; Jabeur, H.; Bouaziz, M.; Sahnoun, Z.
413 Oil from pumpkin (*Cucurbita pepo* L.) seeds: evaluation of its functional properties on wound
414 healing in rats. *Lipids in health and disease* 2016, 15, 73, doi:10.1186/s12944-016-0237-0.

415 19. Medjakovic, S.; Hobiger, S.; Ardjomand-Woelkart, K.; Bucar, F.; Jungbauer, A. Pumpkin
416 seed extract: Cell growth inhibition of hyperplastic and cancer cells, independent of steroid hormone
417 receptors. *Fitoterapia* 2016, 110, 150-156, doi:10.1016/j.fitote.2016.03.010.

418 20. Sanchez-de la Vega, G.; Castellanos-Morales, G.; Gamez, N.; Hernandez-Rosales, H.S.;
419 Vazquez-Lobo, A.; Aguirre-Planter, E.; Jaramillo-Correa, J.P.; Montes-Hernandez, S.; Lira-Saade, R.;
420 Eguiarte, L.E. Genetic Resources in the "Calabaza Pipiana" Squash (*Cucurbita argyrosperma*) in
421 Mexico: Genetic Diversity, Genetic Differentiation and Distribution Models. *Frontiers in plant science*
422 2018, 9, 400, doi:10.3389/fpls.2018.00400.

423 21. Yoeruek, E.; Ziemssen, F.; Henke-Fahle, S.; Tatar, O.; Tura, A.; Grisanti, S.; Bartz-Schmidt, K.U.;
424 Szurman, P. Safety, penetration and efficacy of topically applied bevacizumab: evaluation of
425 eyedrops in corneal neovascularization after chemical burn. *Acta ophthalmologica* 2008, 86, 322-328,
426 doi:10.1111/j.1600-0420.2007.01049.x.

427 22. Rogers, M.S.; Birsner, A.E.; D'Amato, R.J. The mouse cornea micropocket angiogenesis
428 assay. *Nature protocols* 2007, 2, 2545-2550, doi:10.1038/nprot.2007.368.

429 23. Dana, M.R.; Streilein, J.W. Loss and restoration of immune privilege in eyes with corneal
430 neovascularization. *Invest Ophthalmol Vis Sci* 1996, 37, 2485-2494.

431 24. Roshandel, D.; Eslani, M.; Baradaran-Rafii, A.; Cheung, A.Y.; Kurji, K.; Jabbehdari, S.; Maiz,
432 A.; Jalali, S.; Djalilian, A.R.; Holland, E.J. Current and emerging therapies for corneal
433 neovascularization. *The ocular surface* 2018, 16, 398-414, doi:10.1016/j.jtos.2018.06.004.

434 25. Choi, H.; Phillips, C.; Oh, J.Y.; Stock, E.M.; Kim, D.K.; Won, J.K.; Fulcher, S. Comprehensive
435 Modeling of Corneal Alkali Injury in the Rat Eye. *Current eye research* 2017, 42, 1348-1357,
436 doi:10.1080/02713683.2017.1317817.

437 26. Shakiba, Y.; Mansouri, K.; Arshadi, D.; Rezaei, N. Corneal neovascularization: molecular
438 events and therapeutic options. *Recent Pat Inflamm Allergy Drug Discov* 2009, 3, 221-231.

439 27. Edelman, J.L.; Castro, M.R.; Wen, Y. Correlation of VEGF expression by leukocytes with the
440 growth and regression of blood vessels in the rat cornea. *Invest Ophthalmol Vis Sci* 1999, 40, 1112-1123.

441 28. Nakao, S.; Zandi, S.; Lara-Castillo, N.; Taher, M.; Ishibashi, T.; Hafezi-Moghadam, A. Larger
442 therapeutic window for steroid versus VEGF-A inhibitor in inflammatory angiogenesis: surprisingly
443 similar impact on leukocyte infiltration. *Invest Ophthalmol Vis Sci* 2012, 53, 3296-3302,
444 doi:10.1167/iovs.11-8114.

445 29. Kim, Y.M.; Hwang, S.; Kim, Y.M.; Pyun, B.J.; Kim, T.Y.; Lee, S.T.; Gho, Y.S.; Kwon, Y.G.
446 Endostatin blocks vascular endothelial growth factor-mediated signaling via direct interaction with
447 KDR/Flk-1. *J Biol Chem* 2002, 277, 27872-27879, doi:10.1074/jbc.M202771200.

448 30. Gee, E.; Milkiewicz, M.; Haas, T.L. p38 MAPK activity is stimulated by vascular endothelial
449 growth factor receptor 2 activation and is essential for shear stress-induced angiogenesis. *J Cell Physiol*
450 2010, 222, 120-126, doi:10.1002/jcp.21924.

451 31. Koch, S.; Claesson-Welsh, L. Signal transduction by vascular endothelial growth factor
452 receptors. *Cold Spring Harbor perspectives in medicine* 2012, 2, a006502,
453 doi:10.1101/cshtperspect.a006502.

454 32. Han, K.Y.; Chang, J.H.; Lee, H.; Azar, D.T. Proangiogenic Interactions of Vascular
455 Endothelial MMP14 With VEGF Receptor 1 in VEGFA-Mediated Corneal Angiogenesis. *Invest*
456 *Ophthalmol Vis Sci* **2016**, *57*, 3313–3322, doi:10.1167/iovs.16-19420.

457 33. Erdinest, N.; Shmueli, O.; Grossman, Y.; Ovadia, H.; Solomon, A. Anti-inflammatory effects
458 of alpha linolenic acid on human corneal epithelial cells. *Invest Ophthalmol Vis Sci* **2012**, *53*, 4396–4406,
459 doi:10.1167/iovs.12-9724.

460 34. Erdinest, N.; Shohat, N.; Moallem, E.; Yahalom, C.; Mechoulam, H.; Anteby, I.; Ovadia, H.;
461 Solomon, A. Nitric oxide secretion in human conjunctival fibroblasts is inhibited by alpha linolenic
462 acid. *Journal of inflammation (London, England)* **2015**, *12*, 59, doi:10.1186/s12950-015-0104-1.

463 35. Rashid, S.; Jin, Y.; Ecoiffier, T.; Barabino, S.; Schaumberg, D.A.; Dana, M.R. Topical omega-
464 3 and omega-6 fatty acids for treatment of dry eye. *Archives of ophthalmology (Chicago, Ill. : 1960)* **2008**,
465 *126*, 219–225, doi:10.1001/archophthalmol.2007.61.

466 36. Chen, R.; Hollborn, M.; Grosche, A.; Reichenbach, A.; Wiedemann, P.; Bringmann, A.;
467 Kohen, L. Effects of the vegetable polyphenols epigallocatechin-3-gallate, luteolin, apigenin,
468 myricetin, quercetin, and cyanidin in primary cultures of human retinal pigment epithelial cells.
469 *Molecular vision* **2014**, *20*, 242–258.

470 37. Lee, M.; Yun, S.; Lee, H.; Yang, J. Quercetin Mitigates Inflammatory Responses Induced by
471 Vascular Endothelial Growth Factor in Mouse Retinal Photoreceptor Cells through Suppression of
472 Nuclear Factor Kappa B. *International journal of molecular sciences* **2017**, *18*, doi:10.3390/ijms18112497.

473

474